Kinetic and thermodynamic behavior of co-pyrolysis of olive pomace and thermoplastic waste via thermogravimetric analysis

Sánchez-Ávila, N.; Cardarelli, Alessandro; Carmona-Cabello, Miguel; Dorado, M.P.; Pinzi, Sara; Barbanera, Marco

DOI:
10.1016/j.renene.2024.120880

Document Version
Publisher's PDF, also known as Version of record

Citation for published version (Harvard):
Sánchez-Ávila, N, Cardarelli, A, Carmona-Cabello, M, Dorado, MP, Pinzi, S & Barbanera, M 2024, 'Kinetic and thermodynamic behavior of co-pyrolysis of olive pomace and thermoplastic waste via thermogravimetric analysis', *Renewable Energy*, vol. 230, 120880. https://doi.org/10.1016/j.renene.2024.120880

Renewable Energy 230 (2024) 120880

Contents lists available at ScienceDirect

Renewable Energy

journal homepage: www.elsevier.com/locate/renene

Kinetic and thermodynamic behavior of co-pyrolysis of olive pomace and thermoplastic waste via thermogravimetric analysis

N. Sánchez-Ávila [b], Alessandro Cardarelli [a], Miguel Carmona-Cabello [c], M.P. Dorado [b], Sara Pinzi [b], Marco Barbanera [a,*]

[a] Department of Economics Engineering Society and Business Organization (DEIM), University of Tuscia, Largo dell'Università s.n.c., Loc. Riello, 01100, Viterbo, Italy
[b] Department of Physical Chemistry and Applied Thermodynamics, Universidad de Cordoba, Ed Leonardo da Vinci, Campus de Rabanales, Campus de Excelencia Internacional Agroalimentario ceiA3, 14071, Cordoba, Spain
[c] Department of Mechanical Engineering, School of Engineering, University of Birmingham, B15 2TT, Birmingham, United Kingdom

ARTICLE INFO

Keywords:
Agri-food residue
Plastics
Reaction mechanism
Synergistic effect
Valorization

ABSTRACT

This work represents the first attempt to analyze kinetics, thermodynamics and reaction mechanism of olive pomace (OP) and waste plastic materials (PM) co-pyrolysis. Among PM, polypropylene (PP), polystyrene (PS), high density polypropylene (HDPE), polyvinyl chloride (PVC) and poly (ethylene terephthalate) glycol (PETG) were selected. Non-isothermal TG experiments were carried out under inert conditions at four heating rates, namely 5, 10, 20 and 40 °C/min. The kinetic triplet for raw materials and their blends was determined using Starink, Kissinger-Akahira-Sunose and Ozawa-Flynn-Wall iso-conversional models. Pyrolysis mechanism reactions were explained by diverse models, depending on thermal degradation progress. Results shown that co-pyrolysis followed a complex multi-step reaction mechanism. A synergistic effect was detected during co-pyrolysis of OP/PM mixtures. The addition of 50 % (w/w) OP biomass to PM waste decreased the energy of activation (E_a) from 50 to 25 % for all blends, except for PVC/OP. Thermodynamic analysis reveals that adding OP generally reduces the energy barrier (ΔH), except for PS-OP, and improves energy efficiency (ΔG) by facilitating radical formation and molecular chain cleavage.

As a conclusion, this study may open up new avenues for waste valorization and resource recovery. Thus, it may contribute to the transition towards a circular and sustainable economy, through zero waste goal.

1. Introduction

Over the past ten years, the production of municipal solid waste (MSW) has globaly and significantly increased. According to World Bank projections, the yearly output of MSW will quadruple by 2025, starting from 1.3 Mt in 2012 [1].

Synthetic polymers, also known as post-consumer plastic wastes, make up a sizeable portion of all MSW. The volume of post-consumer plastic waste is expected to rise due to an increase in the use of plastic in disposable consumer goods. By 2050, either landfills or the natural environment will receive about 12,000 Mt of plastic waste [2].

Depending on plastic properties and chemical changes it undergoes when heated, they can be classified as thermoplastics or thermosetting plastics. When the temperature reaches a certain point, thermoplastics will melt and can be recast. However, thermoset plastics tend to get harder with rising temperature and cannot be remoulded once formed [3]. Approximately, 80 % of plastics are thermoplastics, mainly used in packaging or textile fibers; about 50 % of them are intended for single use [4]. Thermoplastics, including high-density polyethylene (HDPE), polystyrene (PS), polyvinyl chloride (PVC), polyethylene terephthalate glycol (PETG), polyethylene (PE) and polypropylene (PP), are the most extensively used, i.e. packaging, agriculture, construction, healthcare, electronics and automotive industries [5]. Their success is based on their durability, lightweight properties and cost-effectiveness. Due to their prevalence in municipal plastic waste, thermoplastics are the focus of study. In fact, thermoplastics have become a significant component of MSW [6].

Biomass-derived waste is another type of waste of environmental concern. The olive oil industry produces large quantities of different wastes/by-products, i.e. olive pomace (OP) paste, olive leaves and wastewater, constituting a significant environmental problem, especially in the Mediterranean area [7]. In Spain, the most widespread olive

* Corresponding author.
E-mail address: m.barbanera@unitus.it (M. Barbanera).

https://doi.org/10.1016/j.renene.2024.120880
Received 1 March 2024; Received in revised form 22 June 2024; Accepted 25 June 2024
Available online 26 June 2024

oil extraction process is the two-phase system. Through it, approximately 80 % of the olive mass results in a pomace. This is a dense and viscous substance characterized by a notably moisture content (60–70 %) and composed of olive pulp, skin, crushed pits and residual olive oil [8]. According to the International Olive Council, over 12 Mt of olive pomace are produced annually [9], causing a serious environmental issue due to its phytotoxicity.

Currently, the main OP valorization process is carried out in pomace treatment plants. There, it is transformed to produce “orujo oil” and a solid fuel called "orujo", which is used in direct combustion to generate heat and electricity. This use, however, is linked to the emission of particulate matter and greenhouse gases. Thermal degradation offers an interesting alternative to OP treatment, allowing its degradation into less polluting fuels, including hydrogen, biochar and activated carbons [10].

Pyrolysis is a potential method for harnessing the energy potential of waste materials. This process entails breaking down the waste molecular structure at a moderate pressure and temperature, resulting in a mixture of hydrocarbons in all three physical states. A solid carbonaceous material, bio-oil (a liquid component, with some properties compatible to traditional petroleum-based fuels) and the gas component, which can be utilized to provide energy for the pyrolysis process [11].

However, pyrolysis continues to pose environmental challenges, i.e. gas emissions and energy demand. Nowadays, the use of these wastes as pyrolysis raw materials is minimal. To accelerate the adoption of this waste management solution, policy measures, i.e. subsidies, are essential. In addition, scaling up successful laboratory systems presents challenges that require significant economic investments. However, the potential economic benefits, driven by their commercial applications, justify these investments. Nevertheless, to substantiate this proposal with accurate data, further research on large-scale pyrolysis systems for the management of contaminated mixed plastic waste is needed. Another obstacle to large-scale pyrolysis of contaminated mixed plastic waste is feedstock variability. Improved waste sorting methodologies could facilitate pyrolysis. This may also increase the production of uniform pyrolysis oil, which promises to be a viable substitute for commercial diesel fuel [12].

In recent times, co-pyrolysis of polymers has gained significant attention as a means of upgrading products to valuable hydrocarbon mixtures [13]. This involves the use of more than one type of feedstock mixed together for the pyrolysis process. The use of synthetic polymers with biomass in the co-pyrolysis process can balance the elemental content in the feedstock, resulting in notable effects on the properties of degradation products [14]. Biomass, which has lower thermal stability compared to plastics, can influence the radical degradation mechanism by promoting the degradation of synthetic macromolecules [15].

Exploring future applications of coprolysis of PM and OP biomass, several potential avenues emerge, each offering innovative solutions and sustainable results. One of these is the production of biofuels, such as bio-oil, biochar and syngas. Bio-oil obtained from coprolysis can serve as a renewable energy source, suitable for applications in heat generation, electricity production and transportation fuels. Thus, it may substitute conventional petroleum-derived products, thereby reducing reliance on finite fossil resources and minimizing environmental impacts. On the other hand, biochar derived from coprolysis holds promise as soil amendment. Hence, it contributes to soil health and carbon sequestration. In addition, coprolysis can produce valuable chemical intermediates and chemical platforms with application in different sectors. For example, bio-based polymers, specialty chemicals and value-added products for the agricultural and pharmaceutical sectors. By taking advantage of the unique chemical composition of OP biomass and its synergistic interactions with PM residues, coprolysis opens avenues for the development of new functional materials and additives with improved performance and sustainability credentials.

The useful advancement of co-pyrolysis of lignocellulosic biomass and plastic, as well as scaling-up and equipment design, largely depend on the reaction mechanism and kinetic parameters involved. Thermogravimetric analysis (TGA) is an effective and reliable technique used to both characterize the thermal degradation of solid materials and predict kinetic modelling.

Assessing the feasibility of industrial-scale co-pyrolysis of OP and PM, there are several critical factors. They include feedstock characteristics, operating temperature, residence time, among others previously mentioned for pyrolysis. These parameters collectively influence the scalability and efficiency of the co-pyrolysis process, emphasizing the importance of optimization in reactor design and its industrial implementation.

The International Confederation for Thermal Analysis and Calorimetry (ICTAC) highly recommends the use of iso-conversional methods to determine the kinetic triplet (activation energy, pre-exponential factor and reaction model function) for thermal decomposition processes [16]. Based on ICTAC reccomendations, to evaluate kinetic parameters, Kissinger-Akahira-Sunose (KAS) and Flynn-Wall-Ozawa (FWO) techniques are selected. Meanwhile, Starink method, including both FWO and KAS approaches, is preferred for pyrolysis experiments. This selection is based on its straightforwardness and precision in determining activation energy. These methodologies involve samples at different heating rates. They correlate conversion temperature with heating rate to derive kinetics parameters [17].

Upon careful examination of the available literature, only few studies about co-pyrolysis of OP and plastics has been found. Alcaraz-Ruiz A. et al. [18] studied the influence on dried OP of the inorganic metals inherently present in the ashes obtained during the drying process (K, Na, Ca and Mg) for fast pyrolysis product distribution. Results showed that ashes could be used as catalyst to produce better quality bio-oil. Ouazzani et al. [19] developed a pyrolysis model, to study the efficiency of the co-pyrolysis process of OP and automotive PP-based plastic waste. Results indicated that the co-pyrolysis of OP and plastics enhanced quantity and quality of products compared to straight plastic pyrolysis. Parascanu et al. [20] performed a life cycle assessment of the olive pomace valorization by means of a pyrolysis system. The findings indicated that the pyrolysis system serves as an eco-friendly tool for valorizing olive pomace, utilizing energy-efficient equipment while also recycling water and air.

To gain a better understanding of the co-pyrolysis reaction mechanism, evaluating kinetic and thermodynamic parameters, besides synergistic effects is essential. Therefore, the aim of the current study was to analyze the co-pyrolysis of OP and major thermoplastics (HDPE, PS, PVC, PETG, PE and PP) thus improving the pyrolysis of OP, while simultaneously employing plastic waste. The co-pyrolysis behavior and the extent of the synergistic effect was examined. To determine kinetic parameters, three model-free kinetic methods, namely Starink, Kissinger-Akahira-Sunose (KAS) and Ozawa-Flynn-Wall (OFW) were seleccted. Based on the extent of synergistic effects and activation energy, the most suitable blend sample for co-pyrolysis was identified. Also, to identify the reaction mechanism for the thermal degradation of each sample, the master plot method was used. To the best of our knowledge, this study represents the first attempt to examine the kinetic and thermodynamic analysis, as well as the reaction mechanism, of the co-pyrolysis of OP and plastics waste. These data will allow finding out appropriate reaction temperatures for pyrolysis experiments, laying the theoretical basis for scaling-up.

2. Materials and methods

2.1. Materials and sample preparation

The OP used in this research was sourced from oil mills located in the southern area of Córdoba, Spain. To remove its initial moisture content, OP was lyophilized 48h and further, pulverized and sieved into a fine powder below 200 μm. Plastic wastes, such as HDPE, PP, PS, PETG and PVC, were provided by the Andalusian Plastics Technology Center

(Andaltec, Jaen, Spain). Thermoplastic samples were similarly converted into a powdered form and screened through a sieve; only fractions measuring less than 200 μm were used for the analysis. The resulting powdered biomass and thermoplastic samples were mixed in a 1:1 ratio by weight to provide the blends.

The particle size of the samples was chosen to be below 200 μm to prevent heat and mass transfer effects within the biomass particles. Moreover, when both biomass and plastics possess similar particle sizes, they can be mixed more evenly, leading to an increased contact surface [21].

Sample physicochemical characterization was performed through proximate (moisture, volatile matter, ash and fixed carbon), ultimate (carbon, hydrogen, nitrogen, sulphur and oxygen) and compositional (hemicellulose, cellulose and lignin) analysis. Moisture (M), ash and volatile matter (VM) contents were determined in accordance with EN 14774, EN 14775, ASTM D5630-01, EN 15148 and ASTM D2832-92 standards, respectively. The chlorine content was determined using X-ray fluorescence transmission electron microscope JEOL JEM 1400. Fixed carbon (FC) content was calculated by subtracting the moisture content, ash content and volatile matter, according to ASTM D3173.

Sample ultimate analysis was conducted in the Leco series 928 elemental macroanalyzer (LECO Corporation, St. Joseph, Michigan, US). Oxygen content (O) was determined by difference with all values on a dry basis.

Biomass compositional analysis was conducted according to NREL/TP-510-42618. Additionally, sample high heating value (HHV) was measured according to EN 18125 standard. An IKA calorimeter bomb C200 from Staufen, Germany was used. To ensure result reproducibility, analyses were conducted in triplicate; experimental errors were at ± 3 % of the mean values (Table 1).

2.2. Thermogravimetric analysis

Pyrolysis and co-pyrolysis tests were performed using a TGA DSC 3+ (Mettler Toledo, Barcelona, Spain). Approximately, 25 mg of each sample was pyrolyzed under 50 mL min^{-1} N_2 flow from room temperature to 800 °C [6].

Tests were run out at four different heating rates (5, 10, 20 and 40 °C/min). Heating rates were selected to analyze pyrolysis kinetics under both slow and intermediate heating conditions. From a fundamental perspective, slow heating rates are favored for precise kinetics measurements. Conversely, industrial applications need high heating rates to enhance biofuel quality and economic viability [22]. However, excessively high heating rates can lead to thermal lag and abrupt results, particularly in thermal degradation observed via TGA.

For each test, a blank run using an empty pan to correct for the effects of buoyancy was carried out. Each pyrolysis trial was conducted in triplicate to assess result consistency, yielding deviations below 1 % for all instances. The mean TGA results were used to determine pyrolysis kinetic parameters.

TG and derived thermogravimetric (DTG) curves were continuously recorded as a function of both time and temperature. Then, the curves were studied and analyzed. The thermal behavior, kinetic parameters through various model-free methods and the characteristic indices, namely initial pyrolysis temperature (T_i), pyrolysis-peak temperature (T_p), burnout temperature (T_b) and pyrolysis characteristic index (S), were determined.

T_i is the temperature at which the rate of weight loss reaches 1 % per min after the initial weight loss attributed to moisture content. T_b is the temperature at which the degradation rate reaches 1 % per min at the end of the DTG curve. T_p is the temperature associated with the highest rate of weight loss and provides information about the reactivity of the material as fuel. High values of T_i indicate thermal stability, while high values of T_b mean high difficulty in achieving complete conversion.

To better evaluate the thermal properties of the materials, the pyrolysis characteristic index (S) was calculated according to Equation (1). DTG $_{mean}$ (%/min) denotes the average conversion rate between T_i (K) and T_b (K), determined using Equation (2) [23]. High S reflects good volatile release performance, together with an easy feedstock decomposition. In Equation (2), α_{Tb} and α_{Ti} represent the fractions (%) of the material that undergo degradation at T_b and T_i temperatures, respectively. Variable β (°C/min) represents the heating rate.

$$S = \frac{DTG_{max} DTG_{mean}}{T_i^2 T_b} \tag{1}$$

$$DTG_{mean} = \frac{\alpha T_b - \alpha T_i}{\frac{T_b - T_i}{\beta}} \tag{2}$$

2.3. Kinetic analysis

Thermal decomposition processes of the heterogeneous solid state begin with a devolatilization in the initial stage and involve the liberation of volatiles, which includes light gases and condensable compounds, during the progressive heating of solid material. This release of volatiles is a consequence of the thermal breakdown of the chemical bonds within the natural polymers found in the material, such as hemicellulose, cellulose, and lignin.

To streamline pyrolysis process, the “single step” simplified approach postulates that devolatilization occurs in a single unified reaction. It is based on ICTAC kinetics committee recommendations for analysis of multi-step kinetics [24] using Equation (3) [25]:

$$g(\alpha) = \int_0^{\alpha} \frac{d\alpha}{f(\alpha)} = \frac{A}{\beta} \int_{T_0}^{T} e^{-\left(E_a / RT\right)} dT \tag{3}$$

where g(α) represents the integral form of the reaction mechanism, with the initial condition of α equal to 0 at temperature T_0. β represents the constant heating rate, defined as the derivative of reation temperature with respect to reation time, dT/dt (T and t, in K and min, respectively). α represents the conversion degree during reaction (%) and f(α), the reaction mechanism. F(α) describes how the reaction rate depends on the reaction extent. A is the pre-exponential factor, expressed in s^{-1}. The apparent activation energy is denoted by E_a, measured in kJ/mol. R is

Table 1
Physico-chemical characterization of thermoplastics and olive pomace biomass.

Sample	Proximate analysis (%, m/m)				Ultimate analysis (%, m/m)							Calorific value (MJ/kg)	Compositional analysis (%, m/m)		
	M	VM	Ash	FC	C	H	N	S	O	Cl	H/C	HHV	Cellulose	Hemicellulose	Lignin
PP	0.20	99.45	0.31	0.04	84.23	15.11	–	0.06	0.29	–	0.18	46.14	–	–	–
PS	0.02	99.45	0.19	0.34	91.23	8.35	–	0.05	0.18	–	0.09	40.89	–	–	–
HDPE	0.04	98.73	0.17	1.06	83.68	15.68	0.20	0.15	0.29	–	0.19	46.08	–	–	–
PVC	0.07	95.3	0.0	3.80	42.56	2.65	–	0.33	0.48	53.98	0.06	18.81	–	–	–
PETG	0.39	79.30	0.62	19.69	80.59	13.40	0.50	0.05	5.46	–	0.08	25.39	–	–	–
OP	6.87	67.12	7.64	18.37	48.22	8.05	1.48	0.66	41.59	–	0.17	19.84	23.30	10.70	27.50

PP: Polypropylene; PS: Polystyrene; HDPE: High density polypropylene; PVC: Polyvinyl chloride; PETG: Poly (ethylene terephthalate) glycol; OP: Olive pomace; HHV: High heating value.

the gas constant, which is equal to 8.314 J/mol K.

Table SI 1 (supplementary material) displays the most prevalent reaction models for the decomposition of solid materials, presented in both the differential form, f(α) and the integral form, g(α).

In this study, to evaluate the kinetic parameters, model-free iso-conversional methods, including Starink, KAS and OFW, were used. The OFW method [26,27] (Equation (4)) is based on the application of Doyle approximation [28] to Eq. (3):

$$ln\,(\beta) = ln\left(\frac{AE_a}{Rg(\alpha)}\right) - 5.331 - 1.052\frac{E_a}{RT} \tag{4}$$

For a specific degree of conversion, E_a is provided by the slope of the straight line, derived from the plot of natural logarithm of the heating rate against 1/T. There, T is the reaction temperature at which the specified conversion degree is achieved (K). KAS method is based on the numerical approximation of Murray and White [16], as shown in Equation (5):

$$ln\left(\frac{\beta}{T^2}\right) = ln\left(\frac{AR}{E_a g(\alpha)}\right) - \frac{E_a}{RT} \tag{5}$$

When plotting $\ln(\beta/T^2)$ versus the reciprocal of temperature, 1/T, a linear relationship, with a slope equal to $-E_a/R$, is observed. This enables the determination of E_a. Starink method is a combination of KAS and FWO methods, using a slope of $-1.0008E_a/RT$, as shown in Equation (6):

$$ln\left(\frac{\beta}{T^{1.92}}\right) = -1.0008 \tag{6}$$

2.3.1. Assessment of pre-exponential factors through the energy compensation effects (ECE) method

Iso-conversional methods are effective for precise activation energy values. However, they often lack pre-exponential factor and reaction mechanism information in solid-state reactions. ECE method, however, accurately estimates the pre-exponential factor for single-step reactions. Iso-conversional methods are effective in providing precise values for activation energy. Although, they typically do not yield the pre-exponential factor or the reaction mechanism for solid-state reactions. ECE method, on the other hand, offers a means to accurately estimate the pre-exponential factor for single-step reactions [16]. By applying logarithmic transformations to the differential form of non-isothermal rate law, Equation (7) remains as follows:

$$\frac{d\alpha}{dT} = \frac{A}{\beta}e^{-\left(\frac{E_a}{RT}\right)}f(\alpha) \tag{7}$$

A new expression (Equation (8)) is derived, where i corresponds to a mechanism function listed in Table SI 1 (supplementary material).

$$ln\left(\frac{\beta d\alpha/dT}{f_i(\alpha)}\right) = ln\,A_i - \frac{E_{a,i}}{RT} \tag{8}$$

Plotting the natural logarithm of $[\beta(d\alpha/dT)/fi(\alpha)]$ against the reciprocal of T allows calculation of $\ln A_i$ and $E_{a,i}$ for a given mechanism. A compensation effect is observed when a strong linear relationship between $\ln A_i$ and $E_{a,i}$ under a single heating rate is found. Equation (9) relates $\ln A_i$ to $E_{a,i}$; values of a and b are determined through linear fitting:

$$ln\,A_i = aE_{a,i} + b \tag{9}$$

Starink method, chosen for its accuracy among iso-conversional integral methods, provides activation energies for the compensation formula in Equation (9).

2.3.2. Prediction of reaction mechanism through the master-plot method

The reaction mechanism, f(α), was determined using the master-plot method. Typically, decomposition reactions are quite sluggish at room temperatures. Consequently, the lower limit of the integral on the right side of Equation (3), T_0, can be approximated to zero [29]. The integrated form of Equation (3) can then be expressed as Equation (10):

$$g(\alpha) = \frac{AE_a}{\beta R}\rho(u) \tag{10}$$

where p(u) represents the integral form of temperature and is defined as shown in Equation (11):

$$p(u) = \int_{\infty}^{u} -\left(\frac{e^{-u}}{u^2}\right)du \tag{11}$$

Where u is defined as E_a/RT. The function p(u) does not have an exact analytical solution and as a result, it is solved using numerical approximation methods. Doyle approximation [30] is often applied to provide sufficiently reliable results and can be expressed as shown in Equation (12):

$$p(u) = 0.0048e^{-1.0516u} \tag{12}$$

Considering an a-value of 0.5 as a reference, Equation (10) yields the following result shown in Equation (13):

$$g(0.5) = \frac{AE_a}{\beta R}\rho(u_{0.5}) \tag{13}$$

The ratio of Equations (10) and (13) leads to Equation (14):

$$\frac{g(\alpha)}{g(0.5)} = \frac{p(u)}{p(u_{0.5})} \tag{14}$$

Equation (14) suggests that, for a specific α, the experimental value of p(u)/p(u0.5) and the theoretically calculated one of g(α)/g(0.5) are equivalent when an appropriate kinetic model, f(α), is used. The 15 most common reaction mechanisms are shown in Table S1.1 (Supplementary material).

This integral master-plot method is a valuable tool for determining the reaction kinetic models of decomposition reactions. It allows assessing kinetics of these reactions by comparing experimental data to theoretical ones. This may help elucidating the underlying chemical processes and reaction mechanisms.

2.3.3. Thermodynamic parameters

This study aimed to analyze how thermodynamic parameters change along co-pyrolysis at different conversions. The change in enthalpy (ΔH) between initial reactants and final products indicates that the activated complex required extra energy to convert into the desired product. The change in entropy (ΔS) characterizes the organization and arrangement of molecules within system. A lower value of entropy indicates a more stable system with a more. Change in Gibb free energy (ΔG) shows the availability of energy within the system, including system energy and energy supplied from external sources during pyrolysis and co-pyrolysis process. In agreement with the principles of activated complex theory, the determination of the transition-state entropy is linked to the pre-exponential factor (Eq. (15)).

$$\Delta S = Rln\frac{Ah}{e\chi k_B T_p} \tag{15}$$

where, e is Neper number, χ is transmission factor (assumed as unity for mononuclear reactions), k_B is Boltzmann constant (J/K), h is Planck constant (J s) and Tp is average peak temperature observed from DTG curves at different heating rates.

Transition state theory has been primarily formulated to elucidate the kinetics of monomolecular and bimolecular reactions, occurring within the gaseous phase. Given the intricate network of radical reactions inherent to tar pyrolysis, activation entropy derived from transition state theory ought to be interpreted as an apparent parameter.

This is primarily useful for assessing the heterogeneity of tar. The adoption of this methodology is justifiable upon consideration of solid specific surface (S_{BET}), molecular unit length during decomposition (L) and solid density (ρ), as outlined in Eq. (16).

$$\Delta S = Rln\frac{Ah}{S_{BET}L\rho e\chi k_B T_p} \tag{16}$$

For plastic materials, S_{BET} and ρ were measured by a surface analyzer and a pycnometer, while L is the length of C–C bond ($1.54*10^{-10}$ m). S_{BET}, L and ρ values of OP were assumed from Ref. [31] (Table SI 2). Then, enthalpy changes (ΔH) and Gibbs free energy (ΔG) can be determined by applying Eqs. 17 and 18.

$$\Delta H = E_a - RT_p \tag{17}$$

$$\Delta G = \Delta H - T_p \Delta S \tag{18}$$

2.4. Synergistic effects

To examine the interactions between materials during co-pyrolysis, the additive model was selected. Experimental and calculated values were compared, assuming the absence of interactions between materials [32,33]. Equations (19) and (20) were applied to calculate the deviation ΔM between experimental and calculated TG blend values.

$$M_{calculated} = X_1 M_1 + X_2 M_1 \tag{19}$$

$$\Delta M = M_{experimental} - M_{calculated} \tag{20}$$

where, X_1 and X_2 are the mass fractions of biomass and plastics, while M_1 and M_2 are their corresponding mass values in TG curves of individual materials. $M_{experimental}$ and $M_{calculated}$ are the corresponding mass values of experimental and calculated TG curves.

3. Results and discussion

3.1. Material characterization

To determine their suitability in the process of pyrolysis, physicochemical characteristics of the raw materials were analyzed (Table 1). OP moisture content was below 10 % (w/w), making it viable for use in pyrolysis. As may be seen, OP also contains N and S due to biopolymer composition, i.e. cellulose (23.3 %), hemicellulose (10.70 %) and lignin (27.5 %). Thermoplastics have different compositions, PP, PS and HDPE depicting the highest carbon content (84.23 %, 91.23 %, 70.59 % and 70.58 %, respectively). On the other hand, plastic PETG has a composition rich in carbon (70.58 %) and a significant amount of oxygen (23.76 %) due to the glycerol used in its fabrication. Finally, PVC presents a similar carbon content to that of OP but with less hydrogen or oxygen due to the presence of Cl (54.88 %), which plays an important role in the synthesis reaction. C/H ratio may be an indicator of the pyrolysis process. In this sense, materials rich in carbon and hydrogen produce a higher amount of volatile substances, which enrich the ignition. In this work, two different kinds of thermoplastic ratios were used. The first set shows a higher C/H value, ranging from 0.18 (PP) to 0.19 (HDPE), with over 80 % volatile matter. The second set has ratios ranging from 0.06 (PVC) to 0.09 (PS), with a wider variety of volatile content, ranging from 0.3 % for PVC to 99.45 % for PS. The different C/H ratios will allow a better understanding of synergistic and antagonistic effects, besides improving pyrolysis processes. Finally, the ash content was determined to evaluate the potential for slag and fouling issues, mainly by relating to biomass thermal degradation. Thermoplastic showed values below 1 %, while biomass presented a value of 7.64 %.

In contrast to plastic waste, OP biomass presented reduced levels of volatiles, hydrogen and heating value, though elevated ash and oxygen content. A high volatile matter content offers an advantage during thermal degradation, facilitating vapor formation and subsequent conversion into liquid bio-oil. Due to its intricate composition, lignin is perceived as a constraining element in the thermochemical transformation of biomass. This suggests that agricultural biomass with lower lignin content may be more conducive to thermal degradation and the increased presence of cellulose and hemicellulose in biomass makes it a suitable raw material for co-pyrolysis processes [34].

3.2. Thermal degradation analysis

The pyrolysis behavior of the raw thermoplastic materials, OP biomass and their blends were studied through TGA and DTG curves, as shown in Fig. 1.

As previously reported for individual thermoplastic materials, sample thermograms exhibit a similar inverted S-shape, further confirming the reliability and consistency of products [35–38], . Results obtained are also in accordance with the degree of crystallinity and thermal stability of these polymers. In this sense, HDPE appears as the most thermostable material, due to its highly regular molecular structure and the density of cross-bonds. As depicted in Fig. 1, pyrolysis T_i for the decomposition of PVC is considerably lower than that of other plastics. This lower stability is suggested to stem from the existence of thermally vulnerable structural segments or defects within the polymer chains. Although, the exact cause of PVC's thermal instability remains a topic of ongoing debate, it is widely acknowledged that internal allylic and tertiary chloride segments play a leading role [37].

PP, PS, HDPE and PETG show almost the same trend. It was noted that the degradation of plastics took place within a narrow temperature range. This suggests a rapid breakdown of polymer chains through a one-step mechanism. In contrast, the pyrolysis of PVC exhibits a distinctive two-stage process. The primary mass loss for PVC occurs within the temperature range of approximately 250–390 °C, depending on the material and the presence of stabilizers and additives. During this initial stage, representing a weight loss of approx. 65 %, the primary reaction involves the dehydrochlorination of the polymer, resulting in the formation of HCl PVC and various volatiles [6]. These volatiles predominantly consist of HCl, with minor quantities of benzene, toluene and other hydrocarbons. Subsequently, chlorine is nearly entirely removed during this stage, implying that at low temperatures, most chlorine can be extracted from PVC. The second stage, spanning from 390 to 550 °C, corresponds to the cracking and decomposition of de-HCl PVC.

It is important to note that for PP, PS and HDPE, complete pyrolysis (100 % weight loss) was observed in all tests, which indicates the high purity of the polymer samples, with negligible ash content (as seen in Table 1). For PETG, PVC and OP, a carbonaceous residue of about 10 % (m/m) for PVC and PETG, and 20 % (m/m) for OP remains at the end of the main pyrolysis stage.

DTG curves of the OP samples exhibit three distinct regions, known as water evaporation, active and passive regions. The evaporation phase starts from room temperature and extends to about 140 °C at low heating rates. During this phase, sample water evaporates. The active region spans approximately 130–480 °C for low heating rates and up to 540 °C for higher heating rates. This range is a crucial stage in the pyrolysis process, where devolatilization occurs. In this region, most volatile components are generated, as may be observed by overlapping peaks in the DTG curves. In the process of thermal degradation of olive residue, the lower-temperature peak primarily corresponds to the decomposition of hemicellulose, while the higher-temperature peak primarily is related to the decomposition of cellulose. The peak corresponding to lignin tends to overlap with the other two peaks, as lignin decomposes slowly over a broad temperature range (160–500 °C) resulting in a gradual and gently sloping baseline. That means that due to its higher thermal stability, lignin initiates its decomposition at lower temperatures, like those at which hemicellulose begins to decompose [39]. However, its thermal decomposition range extends to higher temperatures, across the range of both active and passive zones,

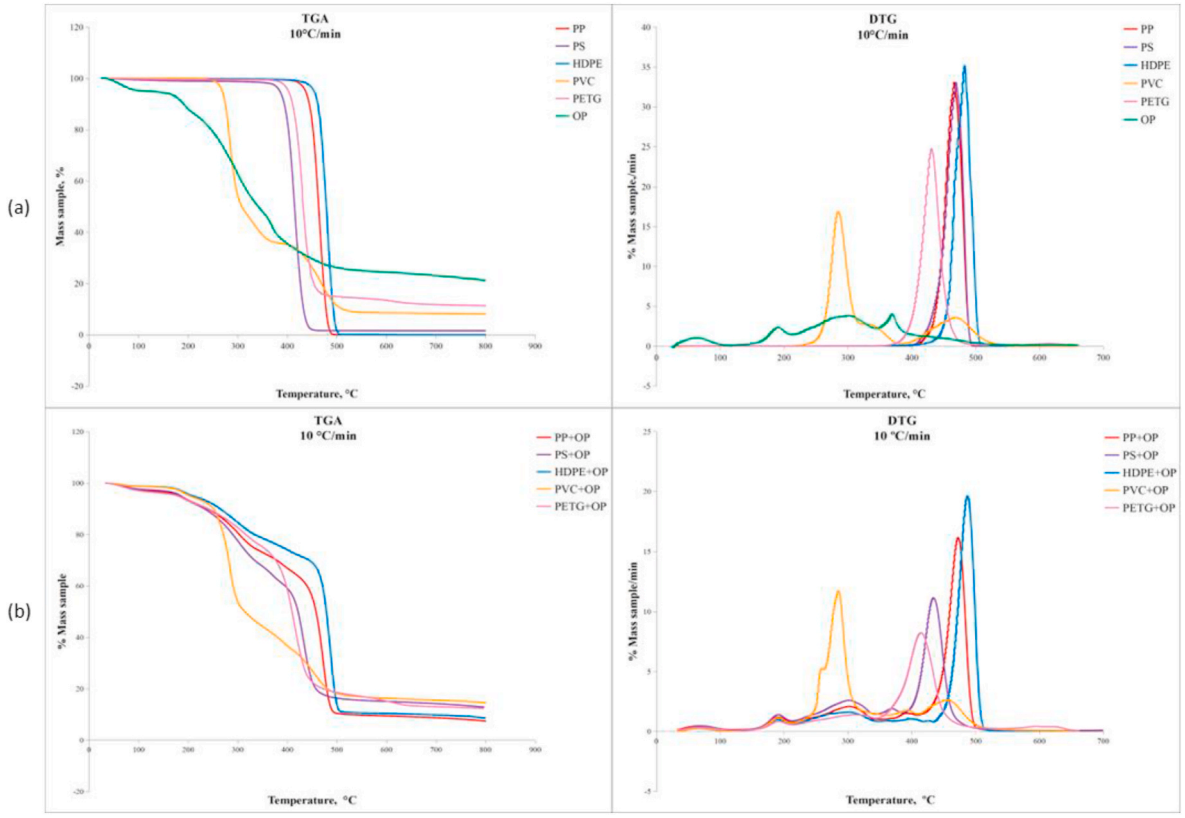

Fig. 1. Pyrolysis conversion (TGA curves) and conversion rate (DTG curves) of the individual materials (a) and their blends (b) at 10 °C/min heating rate.
PP: Polypropylene; PS: Polystyrene; HDPE: High density polypropylene; PVC: Polyvinyl chloride; PETG: Poly (ethylene terephthalate) glycol; OP: Olive pomace; TGA: thermogravimetric analysis curves; DTG: Derivative thermogravimetric analysis curves.

corresponding to the decomposition of heavier volatiles.

According to the literature, thermal degradation of OP biomass and plastic mixtures takes place in two main stages [36]. Lignin, due to its higher thermal stability, triggers decomposition at lower temperatures than hemicellulose, extending to higher ones. Hemicellulose and cellulose predominantly decompose in the initial phase (150–400 °C), influenced by plastic melting. The subsequent stage (350–530 °C) entails the degradation of residual biomass and plastics. Blends exhibit extended primary degradation due to lignin influence, resulting in temperature variations compared to pure materials. As can be seen in Fig. 1, plastics in blends degrade at higher temperatures compared to their pure materials and notably elevate their maximum temperature by 4–20 °C. Whereas, olive residue degrades like pure residues, being its temperature variation less pronounced, ranging from one to 10 °C.This observations highlight the intricate and complex interactions and temperature range involved in the thermal degradation of biomass-plastic blends.

3.2.1. *Effect of heating rate*

Understanding the degradation mechanisms of plastic waste through the influence of the heating rate on the DTG curves and the characteristic pyrolysis parameters may facilitate the improvement of pyrolytic reactor design and, ultimately, lead to the reduction of plastic waste and its recycling in value-added materials.

Figure SI 1 (supplementary material) shows TGA and DTG profiles at different heating rates for each sample. In general, it can be observed that all the curves shift towards higher temperatures as the heating rate increases. This indicates that the increase of temperature rate influences the onset of different pyrolysis stages, resulting in this shift. According to this, a faster heating rate results in a smaller weight loss at specific temperatures. This leads to both an increase in the devolatilization rate and a delay in sample complete combustion, consequently delaying the pyrolysis process. Additionally, the increase in heating rate leads to a more pronounced change in the rate of weight loss, causing at the same time higher yields. Similar previous investigations carried out under non-isothermal conditions align with this behavior, showing that TGA curves shift to higher temperature zones with an increase in heating rate [40].

The low OP thermal conductivity results in a temperature gradient across OP particles, which causes the peaks of the DTG curves to shift. It is expected that at lower heating rates (5 °C/min), where sufficient time for heating is provided, a constant temperature prevails across OP particles, improving heat transfer between them. However, at higher heating rates (10, 20 and 40 °C/min), a significant temperature gradient takes place across OP particle [23]. Another expected fact is the changes in secondary reactions that may occur with varying heating rates. The fastest decomposition rate occurs at high heating rates because of higher thermal energy.

In OP pyrolysis, the amount of residue remaining at the end of the process increases with the rise in heating rates, from 10 to 20 °C/min. This shows that at intermediate heating rates, some compounds may have higher difficulty decomposing completely. High molecular weight compounds, consisting of large and complex molecules, may require more time to completely decompose. At intermediate heating rates, sufficient time may not be provided for these molecules to undergo decomposition. The same trend is found for carbonaceous materials. The formation of solid carbon (char) is common in pyrolysis. At intermediate heating rates, carbon formation is likely to be more significant, as there is insufficient time for complete decomposition of these materials.

3.2.2. *Pyrolysis performance indices*

The analysis of the pyrolysis characteristic parameters is illustrated in Fig. 2, and the corresponding values can be shown in Table 2. The increased heating rate caused the material to reach the required

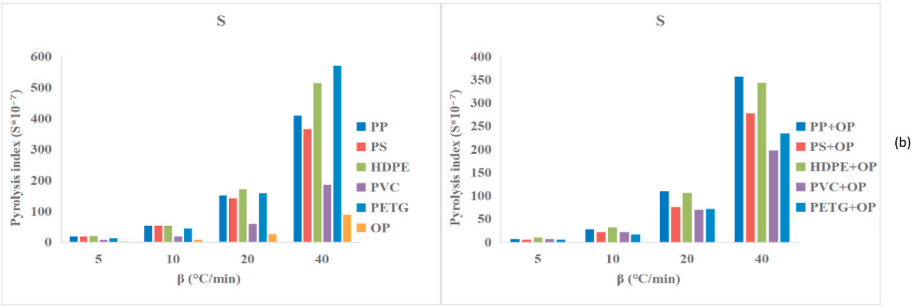

Fig. 2. Comparison of pyrolysis index for each sample of the individual materials (a) and their blends (b), at 5, 10, 20 and 40 °C/min.
PP: Polypropylene; PS: Polystyrene; HDPE: High density polypropylene; PVC: Polyvinyl chloride; PETG: Poly (ethylene terephthalate) glycol; OP: Olive pomace; β: Heating rate; S: Pyrolysis characteristic index.

temperature more quickly, which in turn caused the S, T_p and T_b to shift to higher values. This effect is a consequence of the development of a larger temperature gradient between the interior and exterior of the material and its associated heat transfer limitations. In addition, a higher heating rate slows down the decomposition process, where higher temperatures are less effective compared to lower ones [23].

Data shown in Table 2 emphasize the effect of the mixture of each plastic material with OP biomass on the co-pyrolysis temperatures; T_i, T_p and T_b show an increase with increasing heating rate.

This upward shift in temperatures is attributed to the shorter residence times experienced at higher heating rates. The limited residence time often results in inefficient heat transfer, both within and between particles.

Comparing single materials samples with their OP biomass blends, blending seems to have similar influence on T_i. Though, for the blends, this value is drastically reduced by the influence of the T_i of the first stage of biomass decomposition.

Regarding T_p and T_b, PP, PS and HDPE blends with OP seem to have similar influence, in contrast to PVC-OP and PETG-OP samples, that show less pronounced effects. The values of T_b and T_p for PP, PS and HDPE blends with OP are higher than for individual plastics. The plastic melted and located in char holes, decomposes at a relatively slow rate due to its poor heat conductivity, causing an increase in T_p for plastic decomposition, during the co-pyrolysis process. On the other hand, PVC-OP and PETG-OP blends show a slight reduction in their T_b and T_p values in comparison with their single material.

Fig. 2 shows the comparison of the pyrolysis characteristic index (S) for each sample at the different employed heating rates. It can be observed that the higher the heating rate, the higher the value of S. Raising heating rates sped up the temperature rise, causing T_i and T_b to shift towards higher values. This could potentially improve pyrolysis intensity. Hence, the impact on the blends remains consistent; a reduced heating rate typically leads to a lower S value. At lower heating values, the blends show the following S value trend: PETG < PS < PP < PVC < HDPE. However, for higher heating rates, the trend of S values for the blends is PVC < PETG < PS < HDPE < PP.

3.2.3. *Synergism of co-pyrolysis of waste thermoplastics and olive pomace*

The key to improve bio-oil yield and quality during co-pyrolysis is the synergistic effect. This mechanism may be complex, due to interactions between feedstocks at different mixing ratios and process parameters. Positive or negative synergy depends on the nature and correlation between feedstocks, pyrolysis time, temperature, heating rate, removal of volatile products, catalysts, solvents or hydrogen. Among them, feedstock selection is the most important. Biomass pyrolysis is usually governed by a radical mechanism involving initiation, propagation and termination. However, biomass and plastic copyrolysis mechanism is more complex due to the generation of numerous chemical species. Copyrolysis involve initiation, secondary radical development through depolymerization and monomer generation, hydrogen transfer reactions, intermolecular hydrogen transfer leading to the generation of dienes and kerosenes and isomerization through vinyl groups, followed by termination through radical recombination or disproportionation [41].

The high temperatures of co-pyrolysis of biomass and plastics facilitate radical interactions between resulting products. This interaction leads to the formation of secondary radicals that trigger depolymerization reactions, hydrogen transfer, monomer generation and isomerization. Secondary reactions are pivotal after the initial pyrolysis step. However, their effectiveness is limited when plastics and biomass are pyrolyzed separately. Achieving the optimal plastic-to-biomass ratio is essential for enhancing positive synergies; by balancing carbon-to-hydrogen, carbon-to-oxygen and ash-to-volatile ratios, thereby reducing activation energy requirements. This balance, coupled with optimized physical conditions, can markedly improve product yields like bio-oil, biochar or gas. Thus, it enhances overall process efficiency and product quality from co-pyrolysis [42,43].The potential contribution of hydrogen from plastics during co-pyrolysis may explain the higher yield of desirable products, such as oil and gas [43].

The thermal profiles of Δ M curves of each blend at variable temperatures are showed in Fig. 3. A positive △M value means that observed residual mass of the mixture, the experimental data, is greater than the calculated mass obtained from the individual pyrolysis. Conversely, a negative △M value indicates that the observed residual mass is lower than the predicted value. Therefore, positive △M value denotes a physical hindrance in the degradation of the blends, suggesting negative synergistic interactions between materials. On the other hand, a negative △M means accelerated degradation of the mixtures, indicating positive synergistic chemical interactions. Fig. 3 shows the influence of both polymer and heating rates on behavior. In this sense, PP + OP and PS + OP depict similar behavior. A relative stability up to 200 °C may be found. This may be attributed to encapsulation processes, that increase volatile residence time. From 200 °C onwards, different ΔM responses to temperature ramps are evidenced. Considering PP-OP, negative effects appear above 200 °C; however, at a temperature ramp of 5 °C/min, a positive synergistic effect is found. This may be associated with both melting temperature (160 °C) and volatile release, that increase the degree of free radical reactions. Similarly, PS + OP shows the same behavior at 20 °C/min ramp. This effect may be associated with oxygen concentration, although, for both polymers, it does not exceed 0.30 % (m/m). However, the synergistic effect turns negative from 400 to 500 °C, probably due to inhibition effects of free radical reactions. Furthermore, the H/C ratio is moderate and other processes, i.e. hydrogen transfer inhibition, may occur. Above 500 °C, ΔM decreases below 0 (positive synergistic effect), which may be attributed to both late volatile release and secondary reaction increase. This effect is more evident for PP than PS. For these polymers, adjusting OP/polymer, O/C and H/C ratios positive synergistic effects may increase.

Considering HDPE-OP co-pyrolysis, a general negative synergy

Table 2
Pyrolysis parameters of thermoplastics, olive pomace biomass and their mixtures.

β	Ti	Tb	Tp	DTG max	DTG mean
°C/min	°C	°C	°C	%/min	%/min
PP					
5	419.95	476.23	456.52	18.41	8,66
10	422.17	490.87	466.54	33.08	14,29
20	422.68	506.16	476.70	58.22	23,61
40	423.20	524.49	486.50	99.17	38,83
PS					
5	368.05	432.08	406.79	15.21	7,44
10	372.10	449.92	419.00	26.75	12,47
20	376.66	470.70	430.43	45.39	20,92
40	381.63	494.83	443.27	75.75	34,74
HDPE					
5	428.95	487.47	466.83	21.49	8,28
10	439.00	504.88	483.27	35.20	14,85
20	444.77	520.53	495.44	67.86	26,13
40	447.72	538.85	504.87	127.50	43,60
PVC					
5	252.49	481.45	271.61	12.02	2,03
10	252.79	509.61	285.16	16.86	3,76
20	255.64	536.97	300.07	29.69	6,96
40	260.75	564.48	318.86	54.89	13,01
PETG					
5	379.60	448.94	418.10	12.84	6,49
10	386.31	460.11	430.76	24.76	12,35
20	395.01	479.47	449.93	53.42	22,22
40	402.49	501.38	469.72	120.02	38,59
OP					
5	166.26	371.28	359.36	1.83	1,58
10	170.05	447.60	369.36	4.02	2,91
20	171.54	495.45	307.92	7.42	4,97
40	172.52	556.29	320.31	16.18	9,06
PP + OP					
5	183.2	478.225	459.51	7.16	1.48
10	183.78	495.52	472.591	16.16	2.93
20	186.39	512.186	484.866	34.14	5.74
40	194.21	532.24	499.013	63.17	11.34
PS + OP					
5	180.36	445.79	420.758	5.53	1.62
10	184.21	470.705	434.101	11.13	3.09
20	185.09	501.385	447.071	22.49	5.83
40	187.46	524.152	456.926	44.85	11.42
HDPE + OP					
5	181.27	492.57	475.588	10.73	1.48
10	183.31	508.997	487.256	19.63	2.83
20	185.65	526.693	498.44	35.83	5.40
40	188.13	544.829	510.652	64.20	10.31
PVC + OP					
5	180.68	416.356	272.595	6.02	1.57
10	182.41	488.978	285.047	11.73	2.98
20	186.67	515.712	297.891	22.05	5.68
40	191.4	547.052	311.694	36.98	10.69
PETG + OP					
5	182.43	438.264	403.538	5.55	1.53
10	183.67	460.257	414.248	8.22	3.03
20	185.96	490.362	426.758	20.69	5.83
40	190.87	530.268	440.678	43.85	10.32

PP: Polypropylene; PS: Polystyrene; HDPE: High density polypropylene; PVC: Polyvinyl chloride; PETG: Poly (ethylene terephthalate) glycol; OP: Olive pomace; TGA: thermogravimetric analysis curves; DTG: Derivative thermogravimetric analysis curves; β: Heating rate; DTGmax: Maximum mass loss rate; DTGmean Mean mass loss rate; Ti Initial pyrolysis temperature; Tp: Pyrolysis peak temperature at the maximum mass loss rate; Tb: burnout temperature; S: pyrolysis characteristic index.

behavior is observed, keeping ΔM positive up to 500 °C. This may be due to the late generation of volatiles that may produce an inhibitory effect on the generation of free radicals. The melting temperature of HDPE is around 230 °C; therefore, this effect would partly influence encapsulation. Also, O/C and high H/C composition may be another influencing factor. Above 500 °C, a positive ΔM value, linked to a positive effect, is achieved. This may be associated with the late production of volatiles and, therefore, the emergence of both free radical and secondary degradation reactions. For this polymer, it is unclear whether a variation of OP/polymer or a specific temperature ramp can increase positive synergy.

PVC + OP exhibits a more differentiated behavior, compared to other polymers. This may be due to its high melting point (260 °C) and Cl content (53.18 % (m/m)), among other factors. Above 200 °C, encapsulation effect is observed. Besides, a drastic reduction of ΔM, below zero, is found. This may be attributed to an increase in volatiles, probably due to both free radical formation and the increase in reactions involving C–H, C═C or C═O groups. Also, the high oxygen content of this polymer can play a significant role in the production of reactive species. However, this effect is inhibited between 350 and 400 °C; this may be attributed to the reduction of the number of reactive species, due to the consumption of Cl and O. Above 400 °C, a negative value of ΔM, associated with temperature degradation that generates more volatile elements, is found. Above 600 °C, though, this effect is inhibited.

Considering PETG + OP, a negative synergistic effect takes place from 200 °C to 400 °C. This outcome is probably associated with encapsulation effects. Although, this effect differs at different temperature ramps; 5 °C/min ramps providing faster reduction of ΔM below zero. Above 400 °C, all ramps have a positive synergistic effect, producing a peak between 400 and 500 °C. In this case, it is due to polymer oxygen concentration, derived from the preence of glycerol, which generates free radicals that lead to countless parallel reactions [44].

3.3. Kinetic analysis of co-pyrolysis process

3.3.1. Estimation of the activation energy

E_a is a crucial parameter that characterizes the energy barrier associated with a chemical reaction. It denotes the minimum energy required to initiate a reaction and is key to determine reaction rate reactivity and sensitivity [45,46]. A higher E_a means that more energy is required for the reaction to proceed at a significant rate.

In this study, to estimate the kinetic parameters of the thermoplastics and their blends with OP biomass, three iso-conversional methods (Starink, KAS and OFW) were used. For each method, estimated E_a values for different α and linear correlation coefficient (R^2) are listed in Table SI 3 (supplementary material). According to estimated data, the three model-free kinetic methods successfully determined E_a at different α, showing an excellent fit, with R^2 values mostly exceeding 0.99, which proves the linearity of the iso-conversional curves for each method at each level of conversion.

Fig. 4 reports the trend of the activation energies, obtained by Starink, OFW and KAS for each sample, at each value of conversion degree. As may be seen, the three methods show the same evolution for all samples. Additionally, in the supplementary information (Fig. SI 2), Arrhenius plots using Eq. (4) to (6) for determining E_a, utilizing the Starink, OFW and KAS iso-conversional methods for each sample, are provided. The lines fit across all conversion levels, illustrated in Fig. SI 2, display exceptionally high correlation coefficients, surpassing 0.995, as outlined in Table SI 2. It ensures that E_a values successfully fit the accuracy requirements.

It was observed that, at low conversion rate, OP exhibited lower E_a values than thermoplastics. This suggests that OP biomass possesses lower thermal stability compared to plastics. This may be attributed to the decomposition mechanisms of its primary components, occurring at relatively low temperatures and short reaction times, providing a more efficient process.

OP biomass E_a gradually increases from 100 kJ/mol to 266 kJ/mol, as the conversion extent rises from 0.1 to 0.6, due to the pyrolysis of hemicellulose and cellulose. Then, the E_a value decreases to 255 kJ/mol, as the conversion extent increases from 0.6 to 0.7 for all methods. This is due to the decomposition of a significant portion of lignin and residual cellulose. E_a, within the conversion range of $0.1 \leq \alpha \leq 0.8$, exhibit values ranging from 100 kJ/mol to 270 kJ/mol for Starink, KAS and FWO

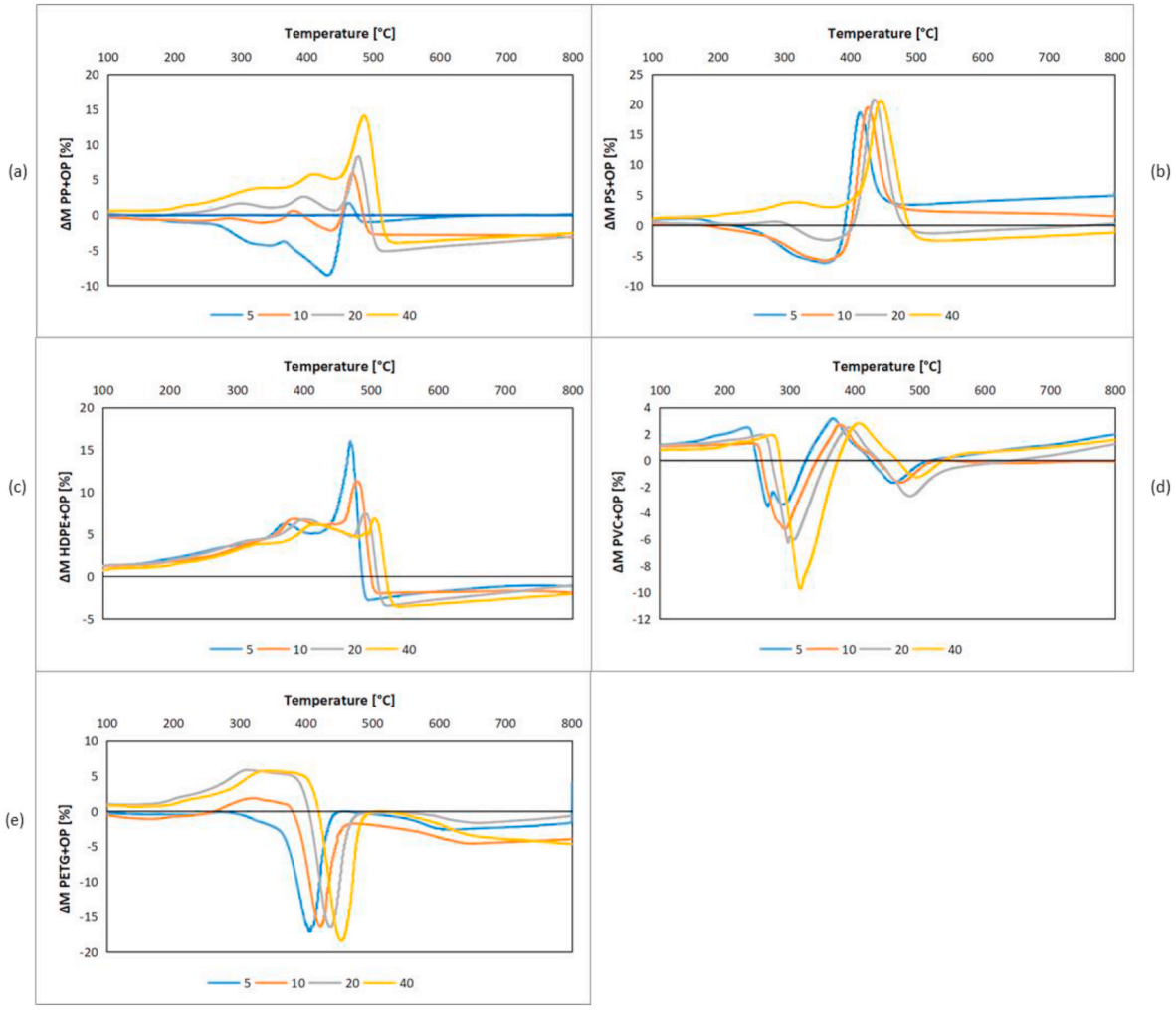

Fig. 3. Difference between measured and calculated thermogravimetric values for each sample at 5, 10, 20 and 40 °C/min; (a) PP + OP, (b) PS + OP, (c) HDPE + OP, (d) PVC + OP and (e) PETG + OP.
PP: Polypropylene; PS: Polystyrene; HDPE: High density polypropylene; PVC: Polyvinyl chloride; PETG: Poly (ethylene terephthalate) glycol; OP: Olive pomace; △M: mass loss difference or deviation between experimental and calculated values.

methods, respectively. Upon reaching a conversion extent of 0.9, E_a decreases to 166 kJ/mol for KAS and 187 kJ/mol for Starink and FWO methods. The average E_a values are 187 kJ/mol for KAS and 189 kJ/mol for Starink and FWO methods.

Owing to the stable structure of polymers, plastics required more energy than OP biomass to initiate the pyrolysis process, as indicated by Ea at lower conversion degrees ($0.1 \leq \alpha \leq 0.4$) listed in Table SI 3. Except for PVC, the rest of the plastics (PP, PS, HDPE and PETG) showed relatively stable E_a values during the whole thermal decomposition process, which is consistent with their thermal degradation mechanism occurring at one-stage. Regarding PVC, the conversion values and trend differs strongly from the other thermoplastics, since its pyrolysis process includes two stages, as observed with the DTG curves. In the initial stage ($0.2 \leq \alpha \leq 0.7$), E_a remains relatively constant, hovering around 120 kJ/mol until the conversion degree reaches 0.7. Subsequently, in the second stage ($0.7 \geq \alpha \geq 0.9$), there is a notable and abrupt rise in E_a, reaching values exceeding 220 kJ/mol. This corresponds to each of the two independent overlapping reactions. The distribution of the average E_a for the raw materials follows the trend: OP < PVC < PETG < PS < HDPE < PP. This is mainly due to bond energy analysis.

E_a is notably affected by α and sample reaction mechanism, being a result of the multi-stage and complex reaction schemes characteristic of the co-pyrolysis process. The value of E_α at the initial stage is relatively small, which indicates that the decomposition of light organic compounds requires low energy.

For PVC-OP blend, a notable interaction was detected during the initial phase of decomposition, whereas the subsequent phase (involving the degradation of hydrocarbons in PVC) was strongly affected. E_a remains near constant at a value close to 120 kJ/mol until reaction reaches the conversion degree of 0.7. Also, E_a sharply increases up to values above 220 kJ/mol, corresponding to every one of the two independent overlapping reactions.

It is worth noting that co-blending biomass with PP, PS and PETG leads to a reduction in E_a compared to that for individual plastic pyrolysis reactions, as reported by numerous studies [37,47–49]. This means that the co-pyrolysis process of these blends requires lower temperature, less energy input and shorter reaction times, making it suitable for various engineering applications. It was determined that the average blend E_a, specifically 149.18 kJ/mol for PP-OP, 131.74 kJ/mol for PS-OP and 138.77 for PETG-OP, were notably lower than those of the individual materials, which were 309.39 kJ/mol for PP, 210.63 kJ/mol for PS and 185.07 kJ/mol for PETG. This fact indicates the existence of a favorable synergistic effect in the combinations of OP biomass and thermoplastics which resulted in a considerable reduction of E_a during the co-pyrolysis process. Burra & Gupta [50] reported a similar trend with the addition of biomass to plastic waste. It was observed that E_a values increased with conversion on account of deterioration of cellulose, hemicellulose and lignin present in OP and the monomers of each

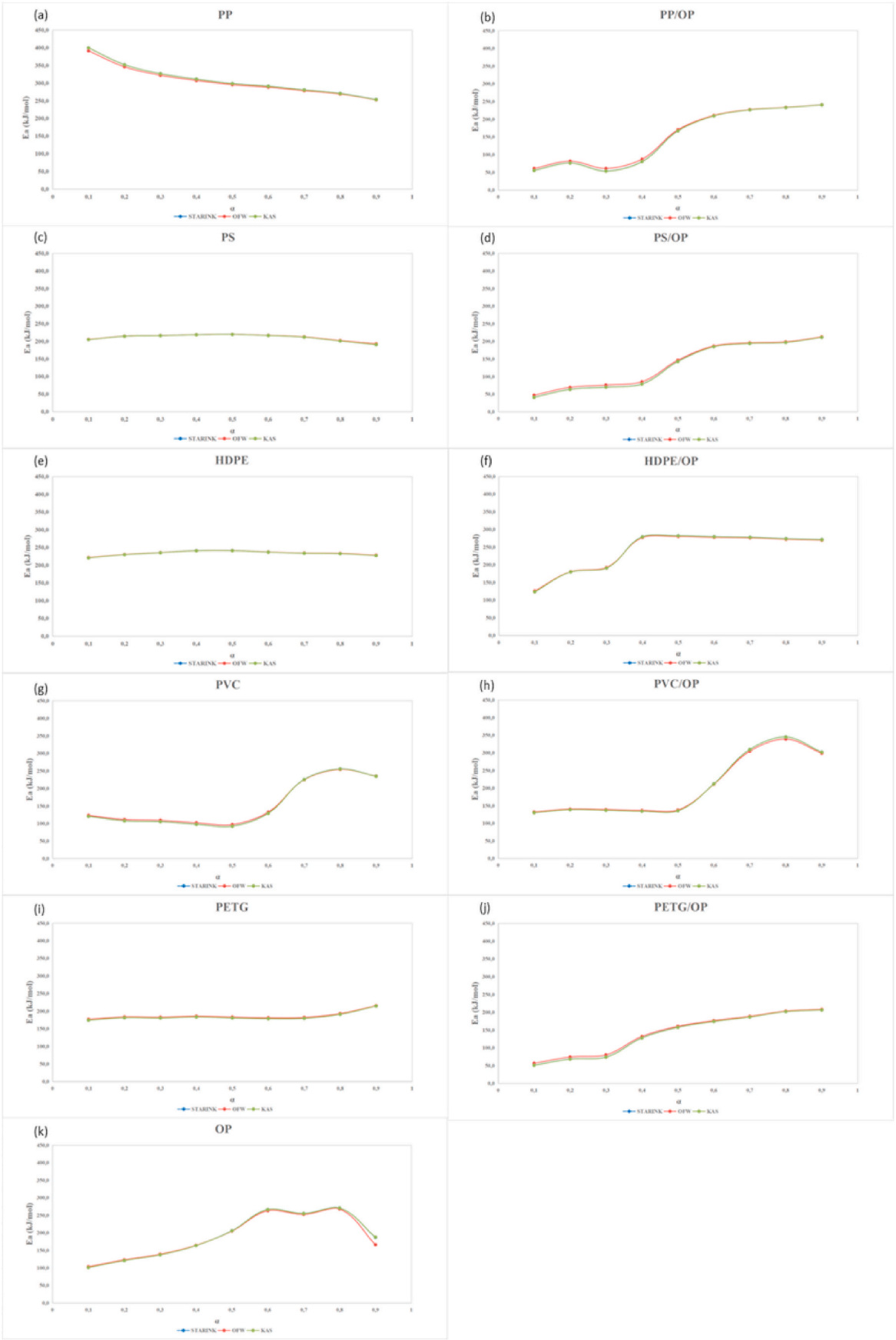

Fig. 4. Evolution of E_a obtained by Starink, OFW and KAS with conversion degree (α) for each raw material (a) PP, (c) PS, (e) HDPE, (g) PVC, (i) PETG, (k) OP, and the blends (b) PP-OP, (d) PS-OP, (f) HDPE-OP, (h) PVC-OP and (j) PETG-OP.

plastic waste (PW) in each case. For HDPE, although, as for the other materials studied, the greatest reduction in E_a occurs at the beginning of the reaction. When comparing the average values obtained for the whole process, HDPE-OP E_a goes up a few units.

The error of kinetic calculations is often derived from the application of multiple methodologies, notably limited to a single due to a general lack of confidence in the obtained results, caused by the nature of mathematical approximations. Within the same set of congruent kinetic methods, an appropriate level of confidence is attainable, allowing for the minimization or exclusion of computational error. In this study, the standard deviation of the average activation energy values was 0.27–1.78 kJ/mol, corresponding to 0.09%–1.34 % on the basis of mean value (Tab. SI 4). Furthermore, deviations of conversion-based E_a values, across a range of conversions from 0.1 to 0.9, were also determined (0.12–3.91 kJ/mol, corresponding to 0.05%–6.40 % on the basis of mean value). Consequently, findings are deemed reliable and accurate, given the notably low standard deviations observed in both average and conversion-based E_a values.

Fig. 4 depicts the evolution of the activation energies obtained by Starink, OFW and KAS with conversion degree, for each sample. The distribution of E_a for blends follows the trend PS-OP < PETG-OP < PP/OP < PVC-OP < HDPE-OP. The iso-conversional methods demonstrated that the co-pyrolysis process required about 50 %, 45 % and 25 % less E_a for PP-OP, PS-OP and PETG-OP than pyrolysis of individual plastic materials.

These estimated E_a values are in agreement with the literature (Table 3). E_a values vary depending on several factors, including heating rate and final temperature, raw material origin and experimental setup. As a result, E_a findings for different feedstocks should only be extrapolated to specific experimental conditions.

PP: Polypropylene; PS: Polystyrene; HDPE: High density polypropylene; PVC: Polyvinyl chloride; PETG: Poly (ethylene terephthalate) glycol; OP: Olive pomace; Ea: Activation energy; α: Conversion degree; KAS: Kissinger–Akahira–Sunose method; FWO: Flynn–wall–Ozawa method.

3.3.2. Assessment of reaction mechanism

Generalized master-plot method was employed to ascertain the reaction mechanism of the pyrolysis of the raw materials, as well as their blend co-pyrolysis. The Starink method was used to calculate the experimental value of p(u)/p(u0.5) across conversion rates ranging from 0.1 to 0.9. The experimental and theoretical values were compared and a correlation factor (R^2) was determined for each model equation, allowing the reaction mechanism of single pyrolysis and co-pyrolysis of plastic and biomass mixtures to be obtained.

Figure SI 3 summarizes the theoretical plots of g(α)/g(0.5) as a function of α and the experimental plots p(u)/p(u0.5), against α, for raw materials and their blends at each heating rate of 5, 10, 20 and 40 °C/min. It was observed that within the range of $0.1 < \alpha < 0.5$, the experimental master plots substantially overlap each heating rate. However, in the range of $0.5 < \alpha < 0.9$, the experimental curves exhibit variations that align with different reaction mechanisms. The appropriate reaction mechanisms were determined by comparing the experimental and theoretical curves within each interval of α. In Table 4, the most suitable reaction mechanisms in the ranges of $0.1 < \alpha < 0.5$ and $0.5 < \alpha < 0.9$ are provided.

Based on the correlation factor, it was observed that thermal degradation of thermoplastics, OP and their blends started with one mechanism model and culminated with another. Pyrolysis reaction of PP follows the geometrical contraction mechanism, R1, mainly in the range of $0.1 \leq \alpha < 0.5$ and R3 in the range of $0.5 \leq \alpha < 0.9$ (Fig. SI 3, supplementary material). HDPE shows same A2 two-dimensional

Table 3
Activation energy values reported in the literature from diverse plastic and biomass samples.

Type of Feedstock	Operartional conditions			Model used	E_a average (kJ/mol)	References
	Heating rate (°C/min)	Final temperature (°C)	Inert gas			
Raw olive wastte	5, 10, 15, 20	900	N_2, 20 mL/min	KAS	202.06	[53]
PS					209.4	
PVC					159.5	
Walnut shells	5, 10, 20, 40		N_2, 20 mL/min	STARINK	158.0	[54]
WS/PS					200.6	
WS/PVC					191.8	
OP	15, 20, 25	500, 600, 700	N_2, 500 mL/min	DAEM	137.1	[55]
Grape steam					191.17	
PW	5,10,15,20	900	N_2, 60 mL/min	KAS	239.76	[46]
GS/PW					183.84	
Bamboo	10, 20, 30 40	700	N_2, 60 mL/min	KAS	180.9	[56]
PP					187.1	
Cherry seed					274.6	
PVC	5, 10, 20, 40	1000	N_2, 20 mL/min	FRIEDMAN	151.5	[57]
CS/PVC					170.8	
Water hyacinth					121.2	
HDPE	15, 25, 35	800	N_2, 40 mL/min	FWO	263.1	[58]
WH/HDPE					206.4	
PS					209.4	
WS					158.0	
Peach Stones	5, 10, 20, 40	1000	N_2, 20 mL/min	STARINK	148.3	[59]
WS/PS					224.2	
Peach Stones/PS					200.6	
PVC					200.49	
PS					204.4	
Thlaspi arvense L. seed	10, 25, 40	900	N_2, 80 mL/min	FWO	239	[38]
TS/PS					223.3	
PS/PVC					200.5	
Pine wood					249.7	
PP	10, 20, 30	1000	Ar, 100 mL/min	DAEM	294.6	[52]
Pine Wood/PP					115.2	

PP: Polypropylene; PS: Polystyrene; HDPE: High density polypropylene; PVC: Polyvinyl chloride; OP: Olive pomace; Ea: Activation energy; α: Conversion degree; KAS: Kissinger–Akahira–Sunose method; FWO: Flynn–wall–Ozawa method; DAEM: Distributed Activation Energy Model; GS: grape steam; WS: Walnut shells; TH: Thlaspi arvense L. seed; WH: Water hyacinth; CS: Cherry seed.

Table 4
Most suitable reaction mechanism in the ranges of $0.1 < \alpha < 0.3$, $0.3 < \alpha < 0.5$, $0.5 < \alpha < 0.7$, and $0.7 < \alpha < 0.9$ for raw and blended materials at 10 °C heating rate.

Sample	$0.1 < \alpha < 0.3$	$0.3 < \alpha < 0.5$	$0.5 < \alpha < 0.7$	$0.7 < \alpha < 0.9$
PP	R1	R1	R3	R3
PS	A2	A2	F1	F1
HDPE	A2	A2	A2	A2
PVC	F6	F6	F10	F10
PETG	A2	A2	F11	F11
OP	F10	F10	F8	F8
PP-OP	F10	F6–F9	R3	R3
PS-OP	F11	D2	D2	D2
HDPE-OP	F5	n.d.	R3	R3
PVC-OP	F5	F5	F11	F11
PETG-OP	D3	D3	D3	F2

PP: Polypropylene; PS: Polystyrene; HDPE: High density polypropylene; PVC: Polyvinyl chloride; PETG: Poly (ethylene terephthalate) glycol; OP: Olive pomace; α: Conversion degree; n.d.: No data.

nucleation mechanism throughout the course of the reaction (Table 4). Similarly, pyrolysis reaction of PS and PETG adhere to A2 two-dimensional random nucleation mechanism, within the range of $0.1 \leq \alpha < 0.5$. In the range of $0.5 \leq \alpha \leq 0.9$, pyrolysis reactions of PS and PETG are predominantly governed by an n-order reaction mechanism, F1 and F11, respectively. At the same time, for PVC and OP, pyrolysis reactions are influenced by n-order mechanism, in the range of $0.1 \leq \alpha < 0.5$, for PVC according to F6 and OP F10, and F10 for PVC and F8 for OP in the range of $0.5 \leq \alpha < 0.9$.

In the case of co-pyrolysis of thermoplastics and OP blends, due to increased interactions, the co-pyrolysis mechanism becomes intricate, and the diffusion (D2, D3), three-dimensional geometrical contraction (R3) and different n-order mechanism models (F2, F5, F6, F8, F9, F10, F11) elucidate the pyrolysis processes (Table 4 and Fig. SI 3, supplementary material).

Analyzing the literature, the pyrolysis mechanisms for OP biomass and thermoplastics differ from those previously reported, as detailed in Table 4. Due to the limited existing studies that provide reaction models for combinations of OP biomass and plastic wastes here studied (PP, PS, HDPE, PVC and PETG), it is not straightforward to make direct comparisons regarding the reaction model. Nevertheless, our findings suggest that introducing OP biomass into plastic wastes modifies the decomposition mechanism of the thermoplastic materials, as can be seen in Figure SI 3 (supplementary material).

3.3.3. *Pre-exponential factor from energy compensation effect*

To determinate the pre-exponential factors, ECE and the previous experimental data obtained for each heating rate, besides Equations (8) and (9), were employed. In Table SI 5 (supplementary material), it may be seen that $E_{a,i,}$ values are associated with various theoretical mechanisms. Moreover, they are notably low, some of them even negative, a trend consistent with the literature [51]. The corresponding plots can be found in Figure SI 4 (supplementary material). Typically, for single-step reactions, ECE results in linear relationships between E_i and pre-exponential factors A_i, as expressed in Equation (8). Remarkably, high linear relationships were observed, with ln (A_i) *vs.* E_i ($R^2 > 0.99$) obtained for all the samples, as depicted in Figure SI 4 and documented in Table SI 5 (supplementary material). This suggests that ECE method accurately estimates the pre-exponential factors for both raw and blended materials. Once the slope and intercept were determined, by using the compensation formula (Equation (9)) and E_a obtained from the Starink method, the pre-exponential factor at each degree of conversion was assessed.

Table SI 6 (supplementary material) shows the values of the energy compensation effects for different samples across α and heating rates of 5, 10, 20 and 40 °C/min. Comparing the fluctuations in the pre-exponential factor for each individual material with α, a high variation for OP biomass is noticed. This may be due to the complexity of its composition and, consequently, the intricate thermal characteristics, in contrast to the simpler polymeric structures of pure thermoplastics. In detail, starting from the initial stages of pyrolysis to the formation of the final products, this variation was caused by the additional energy required to begin the decomposition of hemicellulose and cellulose at the onset of pyrolysis. Once this energy barrier was surpassed, the degradation of OP proceeded with less energy demand.

While for individual raw materials, the average A value calculated with ECE is not significantly affected by the heating rate, for blends the higher the heating rate the lower the A value. These A values are considerably higher than those obtained for all raw materials. Except for PP-OP, the co-pyrolysis for the blends was easier than that of the individual materials. A value of $A > 10^9\ s^{-1}$ means that there are no changes during the rotation of the active complex and reagent in the pyrolysis reaction. Thus, a simpler reaction is determined. So, the higher the A values, the easier the pyrolysis [52].

In detail, all the obtained pre-exponential A values were higher than $10^9\ s^{-1}$ in the range of $\alpha = 0.4$–0.9, indicating that the final stage of decomposition reactions are simple complexes. Thus, more heat is required for higher molecular collision to be transferred, being adjacent to the E_a required. These results agree with E_a characteristics. For PP-OP and PETG-OP, A values were lower than $10^9\ s^{-1}$ in the range $\alpha = 0.1$–0.4, and for PVC and PVC-OP for $\alpha = 0.1$–0.6 and $\alpha = 0.1$–0.5, respectively. This could be associated with a restriction in particle rotation of the activated complex, compared to the initial reagent, showing a large surface reaction.

3.3.4. *Thermodynamic parameters*

In addition to the kinetic triplets, thermodynamic parameters, including variations of enthalpy (ΔH), Gibbs free energy (ΔG) and entropy (ΔS), were determined using E_a values obtained through the Starink model-free method. This method was chosen due to its superior accuracy in calculating E_a compared to other model-free methods. These thermodynamic parameters play a crucial role in the design, scaling and optimization of pyrolysis reactors and processes [53]. Results from Eqs. 16–18 for all heating rates to comprehensively assess their impact are listed in Table SI 7 (supplementary material).

The variation of enthalpy (ΔH) reflects the energy exchange between reactants and products during the reaction process, where the heat is either absorbed or released at a constant pressure. It represents the energy required to break the intricate bonds within biomass, facilitating the formation of new chemical bonds. When the enthalpy variation is characterized by small values, it suggests more favorable conditions for the creation of an activated complex [45]. Furthermore, the minimal energy gap between E_a and ΔH denotes favorable conditions for activated complex generation [55]. It was observed for all materials, except for PS-OP. Average ΔH values were 303, 205, 227, 147 and 179 kJ/mol for PP, PS, HDPE, PVC and PETG, respectively; 143, 205, 233, 199 and 133 kJ/mol for their blends with OP biomass. It is noteworthy that the energy barrier of the blend samples did not rise with increased heating rate.

The fluctuation of Gibbs free energy reflects the overall increase of energy within a system during the formation of the activated complex. Its value serves to evaluate the spontaneity of reactions. A negative ΔG value indicates spontaneous activated complex formation from reagents. Conversely, a high positive ΔG value means low reaction spontaneity. In other words, reactant molecules require more energy to produce activated complexes [56]. In all studied cases, ΔG values were positive. Thus, thermal degradation process did not occur spontaneously, requiring an extra energy during activated complex formation. Additionally, an increase in ΔG was noted within the studied range of conversion degree (Fig. 5) with increasing heating rate. Overall, highest ΔG values were achieved for single materias instead of blends. This suggests that OP presence helps reducing PM-based pyrolysis energy consumption. This effect may be explained by the fact that OP boosts the number

(a)

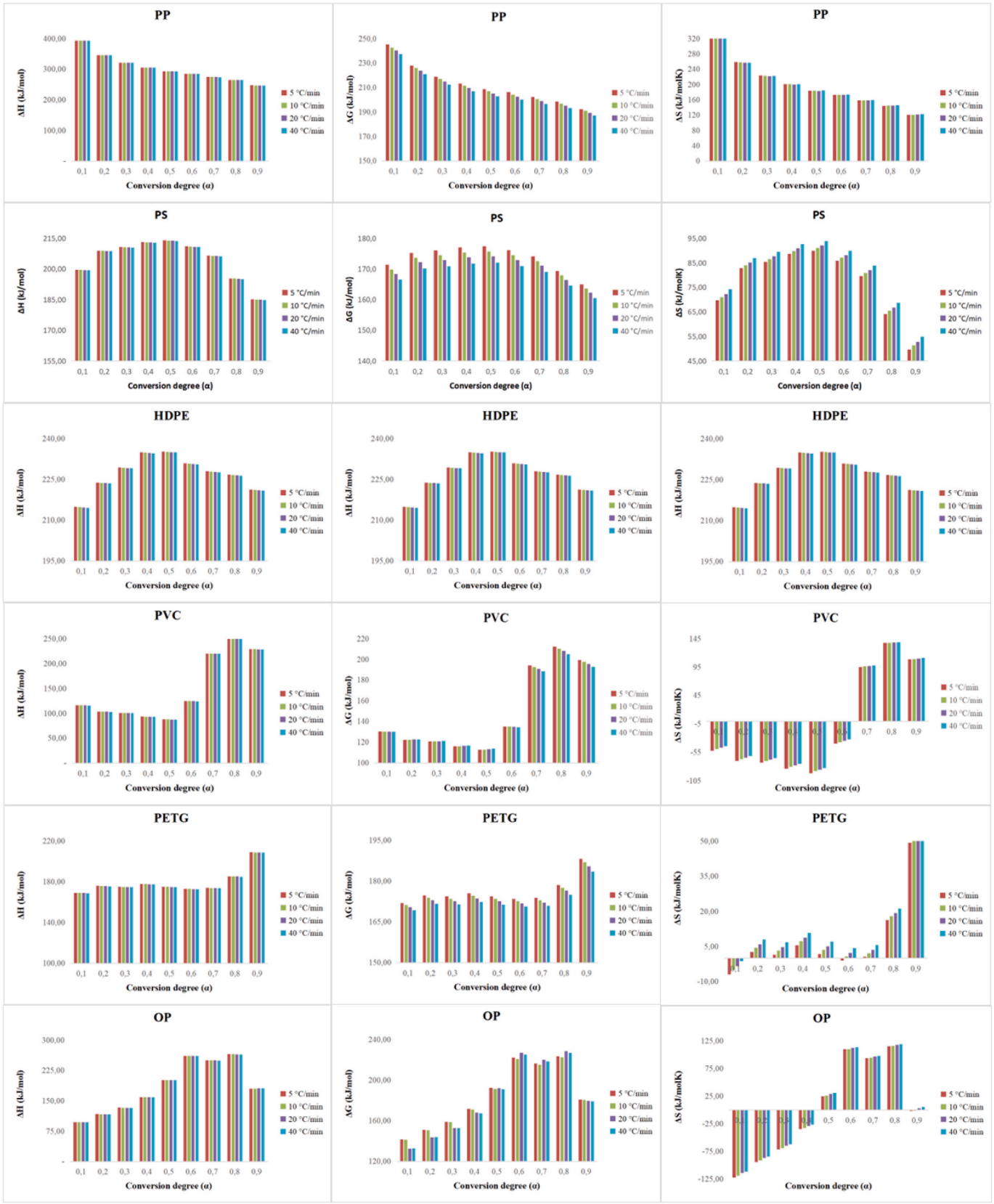

Fig. 5. Thermodynamic parameter variation with conversion degree for: single (a) and blended (b) materials.
PP: Polypropylene; PS: Polystyrene; HDPE: High density polypropylene; PVC: Polyvinyl chloride; PETG: Poly (ethylene terephthalate) glycol; OP: Olive pomace; α: Conversion degree; Avg: Average; A: Pre-exponential factor.

(b)

Fig. 5. (*continued*).

of reactive radicals and promotes the cleavage of WP molecular chains.

ΔS were observed to span negative and positive values for PVC and PP-OP, HDPE-OP, PVC-OP and PETG-OP blends, showing a significant positive increase at the final stage, indicating that the pyrolysis reactivity increases with α. It confirms the complexity of the reactions during their conversion into various products. This is because the dissociation of chemical bonds consumes energy to organize the products. Finally, the products become disordered due to char formation. Negative values of ΔS at lower conversion grades ($0.1 < \alpha < 0.5$) indicate a well-defined alignment of molecules in the activated complex. Lower values of ΔS suggest low reactivity, thus indicating a need for more time in forming the activated complex. Whereas, significant changes in entropy means that the sample is far from thermodynamic equilibrium leading to higher reactivity. This means that the system requires less reaction time to form the activated complex. Thereafter, as α increases from 0.6, the increment of ΔS is mainly associated with further dissociation of cellulose and lignin present in OP and plastic polymers. It is noteworthy that ΔS of blends samples decreased with increased heating rate.

As depicted in Fig. 5 and Table SI 7 (supplementary material), ΔS for PVC and blends previously mentioned goes from negative to positive values with the studied methods.

This means higher system reactivity with conversion. For PP-OP and

PETG-OP blends, ΔH and ΔS values were considerably lower than those showed for single materials, which means that co-pyrolysis process of this materials provides more reactive systems and stable end products, respectively.

Considering Fernandez et al. [57] work on the thermokinetics of pyrogasification of biomass from the food industry, a remarkable difference in the behavior of ΔS values is found. This research consistently reports negative ΔS values throughout the degradation process. In fact, this biomass was subjected to a specific polyphenol extraction process, potentially altering its chemical composition and the nature of volatile release during degradation. However, the present study, focusing on OP and PW mixtures, shows ΔS values changing from negative to positive during degradation. This contrast suggests potential variations in volatile compound release, associated entropy increases and reactivity dynamics between the two types of biomass.

The kinetic and thermodynamic analysis of the pyrolysis of PW and OP blends demonstrates that these materials are viable for pyrolysis conversion due to their energy requirements and thermodynamic suitability. Specifically, the analysis revealed that pyrolysis for all samples is an endothermic and non-spontaneous reaction. Consequently, the thermodynamic analysis results suggest these findings can be used to design and develop thermochemical conversion processes.

4. Conclusions

The present research demonstrates that co-pyrolysis of plastic waste materials (PW) with olive pomace biomass (OP) is an excellent alternative to individual material pyrolysis. In fact, adding OP to PM leads to a considerable reduction in activation energy. OP is a promising source of renewable carbon for generating a wide range of biorefinery products. Besides, PW changes the original reaction model of biomass, leading to an increase in the pre-exponential factor. Pyrolysis characteristic index (S) values depends on heating rate values, thus influencing the type of PW that better behaved. The master plots confirm the diverse kinetic model for each sample as the rate-controlling mechanisms. The synergistic analysis shows that PETG-OP and PVC-OP provide a positive synergistic effect during co-pyrolysis. The thermodynamic parameters shows the feasibility, spontaneity and constant formation of stable products in the co-pyrolysis of PW with OP. Excepting PS-OP, the combination of materials led to a reduction in Gibbs free energy, indicating that OP biomass helps reducing the energy required for pyrolysis of plastics. Average values of enthalpy and entropy for PP-OP and PETG-OP decreased with co-pyrolysis, showing the best performance. In summary, the findings underscore the importance of comprehending the thermo-kinetic and thermodynamic behavior for large-scale co-pyrolysis in bioenergy production. Thus, this research presents a viable solution to reduce the enormous volumes of PW and, at the same time, generate new value-added products. Nevertheless, to evaluate the synergistic impact of varying mixing ratios, additional research is needed. Furthermore, particular attention should be directed towards the analysis of the correlation between OP and PW physico-chemical composition, besides their kinetics under higher heating rates.

Data availability

Data will be made available

CRediT authorship contribution statement

N. Sánchez-Ávila: Writing – original draft, Visualization, Validation, Methodology, Investigation, Formal analysis, Data curation. **Alessandro Cardarelli:** Visualization, Formal analysis, Data curation. **Miguel Carmona-Cabello:** Writing – review & editing, Methodology, Conceptualization. **M.P. Dorado:** Writing – review & editing, Supervision, Funding acquisition, Formal analysis. **Sara Pinzi:** Supervision, Conceptualization. **Marco Barbanera:** Writing – review & editing, Supervision, Data curation.

Declaration of competing interest

The authors declare that they have no known competing financial interests or personal relationships that could have appeared to influence the work reported in this paper.

Acknowledgements

This research was financially supported by the Spanish Ministry of Science and Innovation, through the research projects PID2019-105936RB-C21 and TED2021-130596B–C22. M Carmona-Cabello wants to thank the University of Cordoba for granting Margarita Salas (Next Generation, grant no. UCOR01MS) and Horizon Europe Underwriting by EPSRC (Project no. 1856492). N Sanchez-Avila thanks the Spanish Ministry of Economy and Competitiveness for FPI grant.

Appendix A. Supplementary data

Supplementary data to this article can be found online at https://doi.org/10.1016/j.renene.2024.120880.

References

[1] S. Mariyam, P. Parthasarathy, S. Pradhan, T. Al-Ansari, G. McKay, Co-pyrolysis of biomass and binary single-use plastics: synergy, kinetics, and thermodynamics, Int. J. Sustain. Energy (2023), https://doi.org/10.1080/14786451.2023.2168003.
[2] Z. Murti, Siswanto Dharmawan, D. Soedjati, A. Barkah, P. Rahardjo, Review of the circular economy of plastic waste in various countries and potential applications in Indonesia, IOP Conf. Ser. Earth Environ. Sci. (2022), https://doi.org/10.1088/1755-1315/1098/1/012014.
[3] J. Di, B.K. Reck, A. Miatto, T.E. Graedel, United States plastics: large flows, short lifetimes, and negligible recycling, Resour. Conserv. Recycl. 167 (2021), https://doi.org/10.1016/j.resconrec.2021.105440.
[4] M. Kazemi, S. Faisal Kabir, E.H. Fini, State of the art in recycling waste thermoplastics and thermosets and their applications in construction, Resour. Conserv. Recycl. 174 (2021), https://doi.org/10.1016/j.resconrec.2021.105776.
[5] I.S. Lase, et al., How much can chemical recycling contribute to plastic waste recycling in Europe? An assessment using material flow analysis modeling, Resour. Conserv. Recycl. 192 (2023), https://doi.org/10.1016/j.resconrec.2023.106916.
[6] V. Mortezaeikia, O. Tavakoli, M.S. Khodaparasti, A review on kinetic study approach for pyrolysis of plastic wastes using thermogravimetric analysis, J. Anal. Appl. Pyrol. 160 (2021), https://doi.org/10.1016/j.jaap.2021.105340.
[7] S. Selim, et al., Valorizing the usage of olive leaves, bioactive compounds, biological activities, and food applications: a comprehensive review, Front. Nutr. 9 (2022), https://doi.org/10.3389/fnut.2022.1008349.
[8] R. Aguado, A. Escámez, F. Jurado, D. Vera, Experimental assessment of a pilot-scale gasification plant fueled with olive pomace pellets for combined power, heat and biochar production, Fuel 344 (2023), https://doi.org/10.1016/j.fuel.2023.128127.
[9] J. Dantas Palmeira, D. Araújo, C.C. Mota, R.C. Alves, M.B.P.P. Oliveira, H.M. N. Ferreira, Fermentation as a strategy to valorize olive pomace, a by-product of the olive oil industry, Fermentation 9 (5) (2023), https://doi.org/10.3390/fermentation9050442.
[10] M. Gimenez, et al., Two phase olive mill waste valorization. Hydrochar production and phenols extraction by hydrothermal carbonization, Biomass Bioenergy 143 (2020), https://doi.org/10.1016/j.biombioe.2020.105875.
[11] M. Ma, D. Xu, Y. Zhi, W. Yang, P. Duan, Z. Wu, Co-pyrolysis re-use of sludge and biomass waste: development, kinetics, synergistic mechanism and industrialization, J. Anal. Appl. Pyrol. 168 (2022), https://doi.org/10.1016/j.jaap.2022.105746.
[12] G. Garcia-Garcia, M.Á. Martín-Lara, M. Calero, G. Blázquez, Environmental impact of different scenarios for the pyrolysis of contaminated mixed plastic waste, Green Chem. (2024), https://doi.org/10.1039/d3gc04396g.
[13] J. Choudhary, B. Alawa, S. Chakma, Insight into the kinetics and thermodynamic analyses of co-pyrolysis using advanced isoconversional method and thermogravimetric analysis: a multi-model study of optimization for enhanced fuel properties, Process Saf. Environ. Protect. 173 (2023), https://doi.org/10.1016/j.psep.2023.03.033.
[14] K. Yang, K. Wu, F. Li, L. Jia, S. Wang, H. Zhang, Investigation on the co-pyrolysis of bamboo sawdust and low-density polyethylene via online photoionization mass spectrometry and machine learning methods, Fuel Process. Technol. 240 (2023), https://doi.org/10.1016/j.fuproc.2022.107579.
[15] F.A. Al-Balushi, K.G. Burra, Y. Chai, M. Wang, Co-pyrolysis of waste tyre and pine bark: study of reaction kinetics and mechanisms, Biomass Bioenergy 168 (2023), https://doi.org/10.1016/j.biombioe.2022.106654.
[16] S. Vyazovkin, A.K. Burnham, J.M. Criado, L.A. Pérez-Maqueda, C. Popescu, N. Sbirrazzuoli, ICTAC Kinetics Committee recommendations for performing

kinetic computations on thermal analysis data, Thermochim. Acta 520 (1–2) (2011), https://doi.org/10.1016/j.tca.2011.03.034.
[17] S. Vyazovkin, N. Sbirrazzuoli, Isoconversional kinetic analysis of thermally stimulated processes in polymers, Macromol. Rapid Commun. 27 (18) (2006), https://doi.org/10.1002/marc.200600404.
[18] A. Alcazar-Ruiz, R. Garcia-Carpintero, F. Dorado, L. Sanchez- Silva, Valorization of olive oil industry subproducts: ash and olive pomace fast pyrolysis, Food Bioprod. Process. 125 (Jan. 2021) 37–45, https://doi.org/10.1016/j.fbp.2020.10.011.
[19] W.T. Ouazzani, L. El Farissi, E. Monteiro, A. Rouboa, Automotive plastic waste and olive pomace valorization using the pyrolysis process, Energy Rep. 8 (2022), https://doi.org/10.1016/j.egyr.2022.08.067.
[20] M.M. Parascanu, M. Puig Gamero, P. Sánchez, G. Soreanu, J.L. Valverde, L. Sanchez-Silva, Life cycle assessment of olive pomace valorisation through pyrolysis, Renew. Energy 122 (Jul. 2018) 589–601, https://doi.org/10.1016/J.RENENE.2018.02.027.
[21] X. Wu, Y. Wu, K. Wu, Y. Chen, H. Hu, M. Yang, Study on pyrolytic kinetics and behavior: the co-pyrolysis of microalgae and polypropylene, Bioresour. Technol. 192 (2015), https://doi.org/10.1016/j.biortech.2015.06.029.
[22] G. Ahmed, P.K.R. Annapureddy, N. Kishore, Study on non-isothermal pyrolysis of Azadirachta Indica for kinetic triplets and thermodynamics evaluation, Bioresour. Technol. Rep. 25 (2024), https://doi.org/10.1016/j.biteb.2024.101794.
[23] J. Escalante, et al., Pyrolysis of lignocellulosic, algal, plastic, and other biomass wastes for biofuel production and circular bioeconomy: a review of thermogravimetric analysis (TGA) approach, Renew. Sustain. Energy Rev. 169 (2022), https://doi.org/10.1016/j.rser.2022.112914.
[24] S. Vyazovkin, et al., ICTAC Kinetics Committee recommendations for analysis of multi-step kinetics, Thermochim. Acta 689 (2020), https://doi.org/10.1016/j.tca.2020.178597.
[25] A. Cardarelli, S. Pinzi, M. Barbanera, Effect of torrefaction temperature on spent coffee grounds thermal behaviour and kinetics, Renew. Energy 185 (2022), https://doi.org/10.1016/j.renene.2021.12.116.
[26] T. Ozawa, A new method of analyzing thermogravimetric data, Bull. Chem. Soc. Jpn. 38 (11) (1965), https://doi.org/10.1246/bcsj.38.1881.
[27] J.H. Flynn, L.A. Wall, A quick, direct method for the determination of activation energy from thermogravimetric data, J. Polym. Sci. B 4 (5) (1966), https://doi.org/10.1002/pol.1966.110040504.
[28] C.D. Doyle, Kinetic analysis of thermogravimetric data, J. Appl. Polym. Sci. 5 (15) (1961), https://doi.org/10.1002/app.1961.070051506.
[29] W. Tong, Z. Cai, Q. Liu, S. Ren, M. Kong, Effect of pyrolysis temperature on bamboo char combustion: reactivity, kinetics and thermodynamics, Energy 211 (2020), https://doi.org/10.1016/j.energy.2020.118736.
[30] C.D. Doyle, Estimating isothermal life from thermogravimetric data, J. Appl. Polym. Sci. 6 (24) (1962), https://doi.org/10.1002/app.1962.070062406.
[31] A. Sahoo, S. Kumar, J. Kumar, T. Bhaskar, A detailed assessment of pyrolysis kinetics of invasive lignocellulosic biomasses (Prosopis juliflora and Lantana camara) by thermogravimetric analysis, Bioresour. Technol. 319 (2021), https://doi.org/10.1016/j.biortech.2020.124060.
[32] R. Font, A.N. García, Application of the transition state theory to the pyrolysis of biomass and tars, J. Anal. Appl. Pyrolysis 35 (2) (1995), https://doi.org/10.1016/0165-2370(95)00916-8.
[33] K.R. Vanapalli, J. Bhattacharya, B. Samal, S. Chandra, I. Medha, B.K. Dubey, Inhibitory and synergistic effects on thermal behaviour and char characteristics during the co-pyrolysis of biomass and single-use plastics, Energy 235 (2021), https://doi.org/10.1016/j.energy.2021.121369.
[34] Y. Zhang, Z. Yu, X. Zhang, X. Ma, Comparative study on the synergistic co-pyrolysis of Thlaspi arvense L. seed with different plastics: thermal behaviors, product distributions, and kinetics analysis, Biomass Convers Biorefin 13 (7) (2023), https://doi.org/10.1007/s13399-021-01712-6.
[35] S.A. El-Sayed, M.E. Mostafa, Pyrolysis and co-pyrolysis of Egyptian olive pomace, sawdust, and their blends: thermal decomposition, kinetics, synergistic effect, and thermodynamic analysis, J. Clean. Prod. 401 (2023), https://doi.org/10.1016/j.jclepro.2023.136772.
[36] Z. Ai, et al., Investigation and prediction of co-pyrolysis between oily sludge and high-density polyethylene via in-situ DRIFTS, TGA, and artificial neural network, J. Anal. Appl. Pyrolysis 166 (2022), https://doi.org/10.1016/j.jaap.2022.105610.
[37] T.A. Vo, et al., Co-pyrolysis of lignocellulosic biomass and plastics: a comprehensive study on pyrolysis kinetics and characteristics, J. Anal. Appl. Pyrolysis 163 (2022), https://doi.org/10.1016/j.jaap.2022.105464.
[38] A.A. Shagali, et al., Thermal behavior, synergistic effect and thermodynamic parameter evaluations of biomass/plastics co–pyrolysis in a concentrating photothermal TGA, Fuel 331 (2023), https://doi.org/10.1016/j.fuel.2022.125724.
[39] P. Latko-Durałek, K. Dydek, A. Boczkowska, Thermal, rheological and mechanical properties of PETG/rPETG blends, J. Polym. Environ. 27 (11) (2019), https://doi.org/10.1007/s10924-019-01544-6.
[40] A. Abdullahi Shagali, et al., Synergistic interactions and co-pyrolysis characteristics of lignocellulosic biomass components and plastic using a fast heating concentrating photothermal TGA system, Renew. Energy 215 (2023), https://doi.org/10.1016/j.renene.2023.118936.
[41] M. Alam, A. Bhavanam, A. Jana, J. kumar S. Viroja, N.R. Peela, Co-pyrolysis of bamboo sawdust and plastic: synergistic effects and kinetics, Renew. Energy 149 (2020), https://doi.org/10.1016/j.renene.2019.10.103.
[42] C.C. Seah, et al., Co-pyrolysis of biomass and plastic: circularity of wastes and comprehensive review of synergistic mechanism, Results in Engineering 17 (2023), https://doi.org/10.1016/j.rineng.2023.100989.
[43] Z. Wang, K.G. Burra, T. Lei, A.K. Gupta, Co-pyrolysis of waste plastic and solid biomass for synergistic production of biofuels and chemicals-A review, Prog. Energy Combust. Sci. 84 (2021), https://doi.org/10.1016/j.pecs.2020.100899.
[44] J.N.V. Salvilla, B.I.G. Ofrasio, A.P. Rollon, F.G. Manegdeg, R.R.M. Abarca, M.D. G. de Luna, Synergistic co-pyrolysıs of polyolefin plastics with wood and agricultural wastes for biofuel production, Appl. Energy 279 (2020), https://doi.org/10.1016/j.apenergy.2020.115668.
[45] R. Dong, et al., Co-pyrolysis of vineyards biomass waste and plastic waste: thermal behavior, pyrolytic characteristic, kinetics, and thermodynamics analysis, J. Anal. Appl. Pyrolysis 179 (May 2024) 106506, https://doi.org/10.1016/J.JAAP.2024.106506.
[46] H. Merdun, Z.B. Laougé, Kinetic and thermodynamic analyses during co-pyrolysis of greenhouse wastes and coal by TGA, Renew. Energy 163 (2021), https://doi.org/10.1016/j.renene.2020.08.120.
[47] F. Xu, B. Wang, D. Yang, J. Hao, Y. Qiao, Y. Tian, Thermal degradation of typical plastics under high heating rate conditions by TG-FTIR: pyrolysis behaviors and kinetic analysis, Energy Convers. Manag. 171 (2018), https://doi.org/10.1016/j.enconman.2018.06.047.
[48] R. Chen, et al., Thermal behaviour and kinetic study of co-pyrolysis of microalgae with different plastics, Waste Manag. 126 (2021), https://doi.org/10.1016/j.wasman.2021.03.001.
[49] S. Singh, T. Patil, S.P. Tekade, M.B. Gawande, A.N. Sawarkar, Studies on individual pyrolysis and co-pyrolysis of corn cob and polyethylene: thermal degradation behavior, possible synergism, kinetics, and thermodynamic analysis, Sci. Total Environ. 783 (2021), https://doi.org/10.1016/j.scitotenv.2021.147004.
[50] S. Singh, A. Tagade, A. Verma, A. Sharma, S.P. Tekade, A.N. Sawarkar, Insights into kinetic and thermodynamic analyses of co-pyrolysis of wheat straw and plastic waste via thermogravimetric analysis, Bioresour. Technol. 356 (2022), https://doi.org/10.1016/j.biortech.2022.127332.
[51] K.G. Burra, A.K. Gupta, Kinetics of synergistic effects in co-pyrolysis of biomass with plastic wastes, Appl. Energy 220 (2018), https://doi.org/10.1016/j.apenergy.2018.03.117.
[52] C. Chen, W. Miao, C. Zhou, H. Wu, Thermogravimetric pyrolysis kinetics of bamboo waste via Asymmetric Double Sigmoidal (Asym2sig) function deconvolution, Bioresour. Technol. 225 (2017), https://doi.org/10.1016/j.biortech.2016.11.013.
[53] M.J.B. Fong, A.C.M. Loy, B.L.F. Chin, M.K. Lam, S. Yusup, Z.A. Jawad, Catalytic pyrolysis of Chlorella vulgaris: kinetic and thermodynamic analysis, Bioresour. Technol. 289 (2019), https://doi.org/10.1016/j.biortech.2019.121689.
[54] K. Açıkalın, Determination of kinetic triplet, thermal degradation behaviour and thermodynamic properties for pyrolysis of a lignocellulosic biomass, Bioresour. Technol. 337 (2021), https://doi.org/10.1016/j.biortech.2021.125438.
[55] A.K. Vuppaladadiyam, E. Antunes, P.B. Sanchez, H. Duan, M. Zhao, Influence of microalgae on synergism during co-pyrolysis with organic waste biomass: a thermogravimetric and kinetic analysis, Renew. Energy 167 (2021), https://doi.org/10.1016/j.renene.2020.11.039.
[56] S. Singh, J. Prasad Chakraborty, M. Kumar Mondal, Intrinsic kinetics, thermodynamic parameters and reaction mechanism of non-isothermal degradation of torrefied Acacia nilotica using isoconversional methods, Fuel 259 (2020), https://doi.org/10.1016/j.fuel.2019.116263.
[57] A. Fernandez, et al., Clean recovery of phenolic compounds, pyro-gasification thermokinetics, and bioenergy potential of spent agro-industrial bio-wastes, Biomass Convers Biorefin 13 (14) (2023), https://doi.org/10.1007/s13399-021-02197-z.